J Membrane Biol (2009) 229:153–163
DOI 10.1007/s00232-009-9183-3

Interference of Shot Noise of Open-Channel Current with Analysis of Fast Gating: Patchers do not (Yet) Have to Care

Indra Schroeder · Ulf-Peter Hansen

Received: 7 April 2009 / Accepted: 2 June 2009 / Published online: 24 June 2009

Abstract Microsecond gating of ion channels can be evaluated by fitting beta distributions to amplitude histograms of measured time series. The shape of these histograms is determined not only by the rate constants of the gating process (in relation to the filter frequency) but also by baseline noise and shot noise, resulting from the stochastic nature of ion flow. Under normal temporal resolution, the small shot noise can be ignored. This simplification may no longer be legitimate when rate constants reach the range above 1 μs^{-1}. Here, the influence of shot noise is studied by means of simulated time series for several values of single-channel current of the fully open state and baseline noise. Under realistic optimal conditions (16 pA current, 1 pA noise, 50 kHz bandwidth), ignoring the shot noise leads to an underestimation of the rate constants above 1 μs^{-1} by a factor of about 2.5. However, in that range, the scatter of the evaluated rate constants is at least of the same magnitude, obscuring the systematic error. The incorporation of shot noise into the analysis will become more important when amplifiers with significantly reduced noise become available.

Keywords Beta distribution · Markov model · Microsecond gating · Poisson distribution · Open-channel noise · Rate constant

I. Schroeder · U.-P. Hansen (✉)
Department of Structural Biology, University of Kiel, Leibnizstr. 11, 24098 Kiel, Germany
e-mail: uphansen@zbm.uni-kiel.de

I. Schroeder
e-mail: schroeder@bio.tu-darmstadt.de

Introduction

Ion channels are not permanently open. The process of gating (transitions between conducting and nonconducting conformations of the channel protein) has been the focus of intense research for a long time. Slow gating with time constants in the range of seconds to milliseconds leads to jumps between fixed current levels and can directly be observed in the time series of single-channel patch-clamp experiments. Its evaluation has promoted understanding of the physiological role of channels in medicine (Lehmann-Horn and Jurkat-Rott 1999; Ashcroft 2006) and biology (Blatt 2004; Hedrich and Marten 2006).

To our knowledge, the physiological role of very fast gating in the microsecond range is unknown. Nevertheless, now the analysis of gating beyond 1 μs^{-1} may get new stimuli from the application of molecular dynamics (MD) simulations to ion channels (Compoint et al. 2004; Bernèche and Roux 2005; Miloshevsky and Jordan 2008). There is an increasing demand to test those predictions by physiological measurements. These experiments should yield more than just global parameters like conductivity and selectivity. For instance, evaluating the voltage dependence of the rate constants (1–10 μs^{-1}) of fast flickering in MaxiK channels on voltage and on K^+ concentration led to a model of ion depletion–induced instability of the selectivity filter (Schroeder and Hansen 2007). This could be related to MD simulations indicating that ion depletion causes a transient channel closure due to reorientation of a carbonyl group in the selectivity filter (Bernèche and Roux 2005; Miloshevsky and Jordan 2008).

It is expected that in the near future MD simulations, which have now proceeded to some 10 ns using conventional computer power (Tayefeh et al. 2007; Jeon and Voth

2008), may capture the temporal range above 1 μs when the full state-of-the-art computer power is utilized. For smaller proteins with 30,000 atoms, like Fip35, the range of 10 μs has already been reached (Freddolino et al. 2008), thus giving rise to the hope that the temporal ranges of MD simulations and of physiological gating analysis will more and more overlap. Furthermore, monitoring protein dynamics by fluorescence is of increasing importance (Blunck et al. 2004). It can utilize many of the tools applied for patch-clamp gating analysis, and thus, the considerations below may apply if less than 100 photons reach the detector per lifetime of a conformational state.

Fast gating in the microsecond range can be evaluated only by indirect methods like evaluation of the open-channel noise (Sigworth 1985), based on the feature that the noise found in the conducting state is often stronger than that in the nonconducting state. In records obtained with 10-kHz or 20-kHz filters, rate constants up to 10^7 s^{-1}, i.e., far beyond the filter frequency, have been found (Heinemann and Sigworth 1988, 1990, 1991; White and Ridout 1998; Weise and Gradmann 2000; Schroeder and Hansen 2007, 2008).

Open-channel noise consists of several different components, as listed by Sigworth (1985): (1) baseline noise of the experimental set-up, mainly resulting from the quality of the seal and the noise of the electronic amplifier, the effect on the measured current being determined by the capacity of the pipette and the pipette holder (Levis and Rae 1992; Benndorf 1995; Farokhi et al. 2000; Huth et al. 2008); (2) gating noise (Schroeder and Hansen 2006, 2007, 2008), resulting from fast open–close transitions of the channel, which are smoothed out, but not completely eliminated, by the inevitable low-pass filter of the recording set-up; (3) shot noise, resulting from the discrete nature of electric charge (Schottky 1918).

Once upon a time, i.e., in pre-patch-clamp days (Neher and Sakmann 1976), shot noise played an important role. Analysis of the shot noise of whole-cell recordings with impaled microelectrodes was the only tool for the determination of single-channel current from living cells (reviewed by Neher and Stevens 1977) or from measurements with bilayers (Kolb et al. 1975). Furthermore, it enabled determination of the kinetics of agent-induced channel opening (Katz and Miledi 1970). Other examples of its application in electrophysiology are the effect of the distribution of transporter numbers in liposomes of different size and determination of the apparent rate constants of measured fluxes (Walden et al. 2007). However, this kind of shot noise arose not from stochastic fluctuations related to the transitions of individual ions during an open event but from fluctuations in the number of active channels.

Shot noise caused by the fluctuations in the number of ions passing an open channel (according to the theory of Schottky 1918) was not the focus of analysis because it was hidden by the other two kinds of noise. Only in artificial systems, such as gramicidin A in bilayers, were baseline noise and gating noise so small under certain conditions that shot noise of the open channel became apparent (Heinemann and Sigworth 1988, 1990). Applying the theory of Frehland (1978), this kind of shot noise was included in the analysis. However, there was no explicit study of the influence of shot noise on the determination of the rate constants of the gating process. Such an investigation is presented here because with increasing gating frequencies it becomes questionable whether the exclusion of shot noise is still legitimate for patch-clamp recordings from biological membranes. According to Schottky (1918), the variance of the measured shot noise signal increases with the inverse of the observation time. This is illustrated by the following example. Assume an open-channel current of 16 pA and an open time of 100 ns; then, only 10 ions on average can pass the channel per opening. The Poisson distribution, first applied to the numbers of officers in the Prussian army killed per year by their horses (Bortkewitsch 1898), predicts that the scatter of the number of events equals the square root of the average number of events. This implies for the example that the number of ions passing the channel during an open time of 100 ns is 10 ± 3.

This example illustrates the problem, but it may be misleading. The scatter in ion numbers per open event is not directly relevant for the analysis of fast gating because the low-pass filter of the set-up integrates over the fluctuations from many individual open events. This integrating function of the filter leads to the effect that the shot noise–borne component at the output of the filter is independent of the absolute dwell time of the open events. Thus, in a real experiment it is not the open time of the channel which determines the observation time mentioned in the previous paragraph but the duration of the integrating progress (inverse corner frequency) of the filter. This corresponds to the assumption of Heinemann and Sigworth (1988, 1990) that at constant filter frequency shot noise depends only on single-channel current (Schottky 1918) and not on the gating process.

Nevertheless, the lifetimes of the open events do play an important role, due to another effect: The "noise" resulting from fast gating decreases with increasing gating frequency. Thus, the ratio gating noise/shot noise decreases with decreasing duration of the open events. This, indeed, corrupts the determination of fast gating rate constants as the analysis can no longer distinguish between signals arising from shot noise or from gating noise. In the case of very fast gating, the criterion mentioned by Sigworth

(1985) also does not work, namely, that shot noise results in gaussian amplitude distributions whereas the histograms related to gating are skewed (FitzHugh 1983). This is true for gating not too far above the corner frequency of the filter. However, according to the central limit theorem (Feller 1968), the amplitude histograms of gating noise become gaussian for very fast gating (Schroeder and Hansen 2006, 2007). Furthermore, the magnitude of shot noise cannot be estimated from channel-free sections of the time series as it can in case of baseline noise. However, it could be calculated from a theoretical equation (Schottky 1918; Sigworth et al. 1987), as described below.

A very sophisticated approach to separate these different kinds of noise has been used for gramicidin A channels using the spectral densities of noise (Heinemann and Sigworth 1990) or higher cumulants of amplitude histograms (Heinemann and Sigworth 1991). These analyses were based on an analytical approach using some useful approximations of the underlying mathematical relationships. In contrast, we base our analysis on amplitude histograms (beta distributions) generated from simulated time series. The usage of surrogate time series with several millions of data points has become possible by the progress in available computer power. The benefits are incorporation of the exact filter response and the options of using multistate Markov models of gating and scaling the shot noise. Scaling may become necessary since the variance of the shot noise as calculated from the net current can be decreased by the occurrence of single-file diffusion and/or of cascaded processes (Heinemann and Sigworth 1990; Piccinini et al. 2007) or increased by high unidirectional fluxes (Piccinini et al. 2007). The most important benefit, however, is that Markov models with more than two states can be used if necessary. For instance, spectral analysis of noise provides just one number, i.e., the zero-frequency limit of the spectral density (Heinemann and Sigworth 1988). Analysis of amplitude histograms by means of cumulants (Heinemann and Sigworth 1991) yields two numbers, i.e., mean duration of pulses and mean frequency of the occurrence of ion transitions. In contrast, recent investigations of the amplitude histograms obtained from MaxiK channels revealed three fast gating processes with rate constants higher than the corner frequency of the 20-kHz filter, very short and short closures interrupting the main open state and short openings interrupting the main closed state (i.e., six parameters for fast gating and two for slow gating) (Schroeder and Hansen, unpublished data).

Here, we report on results from these simulations that reveal up to which order of magnitude rate constants can be evaluated in the presence of a given baseline noise and in which range the analysis of gating may suffer from the interference of shot noise.

Materials and Methods

Definitions

Open-channel noise is the noise measured during the open state of a channel. It consists of three components: baseline noise, gating noise and shot noise.

Baseline noise (σ_B) includes all sources of noise which contribute to the noise in channel-free patch recordings. Often, the noise measured in the closed state is used as baseline noise, but is has to be mentioned that also the apparent closed state, e.g., in MaxiK channels, can include undetected fast gating in the form of very short open events (I. Schroeder and U.-P. Hansen, unpublished data).

Shot noise is the noise which results from the discrete nature of electric current, as given by the fact that the electric charge of an ion is an integer multiple of $1.6{\cdot}10^{-19}$ As. The ratio between the variance σ of the shot noise and the mean value of the current i_0 is given by the Fano factor (Fano 1947):

$$F = \frac{\sigma^2(n)}{n_0} = \frac{\sigma^2(i)}{e i_0} \tag{1}$$

with n being the number of ions and n_0 the expected value.

Most well-known is the case $F = 1$; i.e., the shot noise is determined by the Poisson distribution of the numbers of ions passing the channel during a fixed time interval (Schottky 1918). This holds if the movement of ions is statistically independent (no single-file diffusion, no jumps across multiple energy barriers) (Heinemann and Sigworth 1990; Piccinini et al. 2007) and if the net current i_0 is equal to the unidirectional current (Piccinini et al. 2007).

i_0 (equal to I_{true} in Hansen et al. 2003) is the current flowing through the channel during an open event of such a length (often hypothetical) that the statistical limit is reached, thus excluding the interference from shot noise and filter effects. Below, i_0 is related to the expected number of ions passing during an individual open event.

I_{app} is the apparent current measured at the output of the low-pass filter. It is equal to or less than I_{true} (i_0) due to averaging over open and closed times. This is defined in more detail by Hansen et al. (2003).

Gating noise results from fast gating. If the rate constants of gating are larger than the corner frequency of the inevitable low-pass filter of the set-up, then the open and closed transitions no longer reach the full nominal levels but lead to a signal scattering around I_{app}. The amplitude histograms related to fast gating are described by beta distributions (FitzHugh 1983; Yellen 1984). Beta distributions are skewed at rate constants not too far above the corner frequency of the filter and become more and more

gaussian (Schroeder and Hansen 2006) with increasing rate constants due to the central limit theorem (Feller 1968).

Data Simulation

There is no simple analytical algorithm for the calculation of beta distributions for a given Markov model if the order of the filter is greater than 1 (Riessner 1998). Thus, time series and the corresponding amplitude histograms were simulated by the program simulat_p (available at www.zbm.uni-kiel.de), which employed the KISS generator (Marsaglia 2003) for the creation of uniformly distributed random numbers.

The simulation algorithm is similar to that of Gillespie (1977). It is described by Schroeder and Hansen (2006). Briefly, the generation and filtering (by a digital four-pole Bessel filter with a corner frequency of 50 kHz) of the time series were done in continuous time. This allowed dwell times much shorter than the sampling interval (5 µs throughout this article). Simulations started from a given Markov model with a given set of rate constants k_{ij}. A pair of random numbers was generated for each transition in the Markov model: The first one selected the sink state of the next transition as weighted by the related rate constants. The second one determined the time of the next jump calculated from the inverted dwell-time histogram.

New in this latest version of the program was a third random number that was generated for each open event in order to account for the shot noise. There may be three different approaches. (1) The variance of the shot noise depends on the time constant of the low-pass filter and on the average current (see also discussion of Fig. 2c, below). The resulting gaussian distribution could be convoluted with the open-point distribution obtained from the time series simulated by the routine described above. (2) The stochastic sequence of ions through the channel can be presented by delta peaks (Frehland 1978; Heinemann and Sigworth 1988). (3) For open times shorter than the time constant of the filter, it is sufficient to use square-wave pulses with the length of the related open-event. This square wave has to contain the same charge as the series of delta pulses per open event (see Fig. 1a). The statistics are implemented by variable heights of the pulses. The square-wave approach shortens computing time by a factor that is roughly equal to the average number of ions passing per average open event. This approach was implemented as follows. From the actual dwell time in the open state T and from the nominal average true single-channel current i_0, the expected number of ions n_T passing the channel during this event was calculated as follows:

$$n_T = i_0 T/e \tag{2}$$

with e being the elementary charge. However, n_T is different from n, the number of ions actually passing the

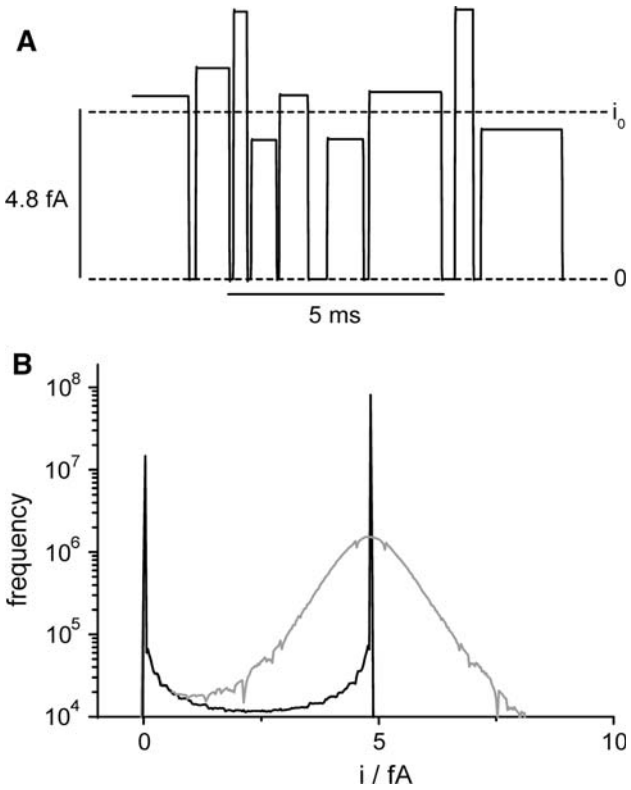

Fig. 1 The influence of shot noise ($F = 1$, Eq. 1) in a hypothetical situation. A time series was simulated with negligible smoothing by the 50-kHz four-pole Bessel filter. With $k_{OC} = 10^3\ s^{-1}$ ($k_{CO} = 5{\cdot}10^3\ s^{-1}$), i_0 had to be 4.8 fA in order to fulfill the condition that on average 30 ions pass the channel during an open event (Eq. 2). **a** Variability of charge transported per individual open event schematically presented as averaged current i times dwell time in the open state (Eq. 2). *Dashed lines* denote the baseline (*lower*) and i_0 (*upper*). **b** Amplitude histogram created from the time series simulated with (**a**, *gray*) and without (not shown in **a**, *black*) shot noise. Sampling frequency was 200 kHz

channel during the opening of length T. Using the random number $r \in [0, 1]$, n was calculated from the Poisson distribution by means of the inverse transform method (Devroye 1986). Starting with $p_1 = 1/\exp(n_T)$ for $j = 1$, the Poisson probability distribution

$$p_j = \frac{n_T^j}{j!} e^{-n_T} \tag{3}$$

was calculated for increasing values of j, until the cumulative probability function P_n exceeded the random number r:

$$P_n = \sum_{j=1}^{n} p_j > r \tag{4}$$

From the resulting n, the individual current value i for this open event is calculated via an inversion of Eq. 2 (after replacing n_T by n and i_0 by i). The resulting time series is then subject to filtering, prefiltered noise is added and the result is sampled at 200 kHz.

Schroeder and Hansen (2006) have shown that in many cases the evaluation of fast gating in a multistate Markov model can be separated from the evaluation of slow gating by using the open-point histogram (distribution per level) (Schroeder et al. 2004). For instance, in MaxiK channels, three gating processes were found with rate constants higher than the low-pass filter of the recording set-up (20 kHz). In most cases, the fastest transition process could be evaluated by means of a two-state model without much interference from the other two processes (I. Schroeder and U. P. Hansen, unpublished data). Because of these findings and because only basic principles are to be investigated here, time series were simulated from two-state Markov models:

$$C \underset{k_{OC}}{\overset{k_{CO}}{\rightleftharpoons}} O \tag{5}$$

k_{CO} was set to $5 \cdot k_{OC}$ in all simulations with different absolute rate constants, different average true single-channel currents i_0 and different baseline noise σ_B. This caused a realistic reduction of the apparent open-channel current I_{app} to 80% of the true single-channel current $I_{true} = i_0$ (Schroeder and Hansen 2006, 2007).

Results

Figure 1a shows a time series which has been simulated on the basis of the C-O model in Eq. 5 without any baseline noise and without significant influence of the filter. This holds at very low gating frequencies, far below the corner frequency of the anti-aliasing filter. The open-channel current i_0 flowing during the open event of time T is a hypothetical average value calculated from the transported charge ne_0 by means of Eq. 2. Interestingly, there are many pulses with amplitudes far above the nominal single-channel current i_0.

The situation depicted in Fig. 1a is a schematic presentation of the parcels of charge flowing during an actual opening event. The square waves in Fig. 1a cannot be observed in real experiments. Besides the problem of having a noise-free amplifier, a very sophisticated recording apparatus is required (an integrator which is activated exactly for the time T of the actual open event). Presenting the averaged current i_0 instead of single delta pulses is done for two purposes. First, the ion flow per open event occurs as a series of stochastically spaced delta peaks. Such a picture hardly gives any estimation of the shot noise–induced variation of the parcels of charge provided per open event. Second, in real records, the filter integrates over the whole response time of the filter. Thus, it does not matter whether the charge is delivered by single delta pulses or as a parcel containing the total charge of these

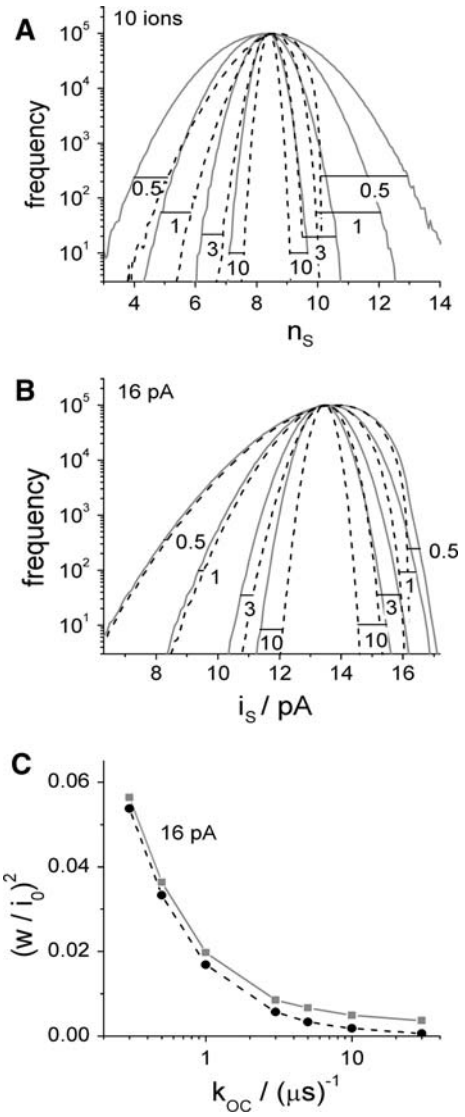

Fig. 2 Amplitude histograms obtained from time series simulated from a C-O model (Eq. 5) in the absence of baseline noise with the rate constants $k_{OC} = x$ µs^{-1}, with x given in the figures, and $k_{CO} = 5 \cdot k_{OC}$. i_S is the simulated current as "recorded" at the sampling times, and n_S is calculated from i_S by means of Eq. 2. *Gray solid curves* were obtained with shot noise ($F = 1$, Eq. 1) being included in the simulations, whereas it was excluded for the *dashed black curves*. *Horizontal bars* labeled with k_{OC} (in µs^{-1}) connect histograms obtained under the same conditions with and without accounting for shot noise. **a** The common parameter of all curves is $n_0 = 10$ (Eq. 2). **b** The nominal open-channel current is constant ($i_0 = 16$ pA). The sampling frequency was 200 kHz, and the corner frequency of the four-pole Bessel filter was 50 kHz. **c** Plotting normalized (to i_0) w^2 (w = FWHM = width at 50% of maximum value of the histograms, Eq. 7) vs. k_{OC} shows that shot noise (difference between the *solid* and *dashed curves*) is independent of k_{OC}

delta pulses. This becomes obvious in more detail in Fig. 2c.

In Fig. 1b, the amplitude histogram resulting from the time series in Fig. 1a (gray) is compared with that

generated without shot noise (but under otherwise the same conditions, black). Because of the absence of baseline noise and of a significant effect of the filter, the histogram of a shot noise–free process consists of two narrow peaks at the nominal open and closed levels. The points between the peaks result from noninfinitely fast transitions between the open and closed levels, indicating a residual effect of the filter with a very high corner frequency.

If shot noise (Fig. 1a) is included, the open-point histogram becomes broader but not the closed-point histogram (the square root of zero is zero, Eq. 1). In contrast to the effects of fast gating (dashed lines in Fig. 2) (Schroeder and Hansen 2006), shot noise generates pulses also with amplitudes higher than the nominal value (Fig. 1a) and, thus, causes the long slope at single-channel currents higher than i_0. Furthermore, the open-point distribution takes a symmetric shape.

The situation in Fig. 1 is not only unrealistic due to the absence of baseline noise. Even more serious is the small magnitude of single-channel current used in the simulation. Elimination of the influence of the filter requires rate constants in the range of milliseconds and consequently very low single-channel currents in the range of femtoampere according to Eq. 2 (i.e., a factor of 10^3–10^4 below the currents in MaxiK channels considered below). Such small currents cannot be measured with current patch-clamp setups. The noise resulting from fast gating and/or from the recording apparatus is much higher than the shot noise related to the Poisson distribution. Thus, there is no chance that the shot noise becomes apparent from a visual inspection of time series such as the hypothetical one in Fig. 1a. Because of this, the analysis has to be based on processed data as provided by spectral densities (Heinemann and Sigworth 1988) or amplitude histograms (Heinemann and Sigworth 1991; and investigations here).

Figure 2 shows amplitude histograms of fast gating time series simulated with and without shot noise (Eq. 1). These simulations were still done without electronic baseline noise in order to study the interplay between the effects of fast gating and of shot noise. The influence of fast gating on the amplitude histograms (as shown by the black dashed lines in Fig. 2a, b) has been described recently (Schroeder and Hansen 2006). One important feature is the shift of the peak of the histogram from i_0 at 16 pA to I_{app} at the highest gating frequency (Fig. 2b). If the gating frequency is high enough, I_{app} is at 13.3 pA according to the equation

$$I_{app} = \frac{k_{CO}}{k_{CO} + k_{OC}} i_0 \tag{6}$$

Here, we concentrate on the influence of shot noise. In the simulations, mean open times ranged between 33 ns and 1 ms, but in Fig. 2 only the interesting range between 100 ns and 2 μs is presented, by four curves each.

At lower gating frequencies, the histograms without shot noise become more and more skewed, with a soft slope toward the closed level. At the open level, there is a rapid drop because the current cannot exceed the nominal value i_0 ($k_{OC} = 0.5$ and 1 μs^{-1}). With shot noise, the histograms take a more symmetric shape because current values above i_0 become frequent (Fig. 1).

In Fig. 2a, the constant parameter is $n_0 = 10$, i.e., the average number of ions per average open time $\tau_0 = 1/k_{OC}$. Under this condition, mean open time τ_O and average single-channel current i_0 are related by Eq. 2. Thus, the values of $i_0 = 0.8$, 1.6, 4.8 and 16 pA correspond to $k_{OC} = 0.5$, 1, 3 and 10 μs^{-1}, respectively. Histograms with (gray solid lines) and without (black dashed lines) shot noise, which have been obtained with the same gating rate constant k_{OC}, are linked by two horizontal bars. According to the central limit theorem (Feller 1968), the distributions approach a gaussian shape if gating becomes much faster than the corner frequency of the filter. This is found for the curves for 3 and 10 μs^{-1}. Then, the effect of shot noise can be adequately described by mere broadening of the histograms.

In Fig. 2b, the constant parameter is the nominal single-channel current i_0. (The pair of curves for $k_{OC} = 10$ μs^{-1} is the same as in Fig. 2a.) However, now, the differences between the histograms with and without shot noise decrease with decreasing gating rate constants. In order to fulfill Eq. 2, n_0, the average number of ions passing per open event, increases with the mean open time $\tau_0 = 1/k_{OC}$.

In Fig. 2c, the square of the full width at half maximum (FWHM) of the histograms is plotted vs. the rate constant k_{OC} (FWHM = 2.354 σ in the case of gaussian distributions). FWHM is also called w here in order to have a short term in the graphs and in the equations below. The conditions are those of Fig. 2b, i.e., $i_0 = 16$ pA = constant, bandwidth = 50 kHz, no baseline noise. Plotting the square of the width leads to parallel curves for histograms including only w^2_{gating} (black, dashed) and for those with additional shot noise w^2_{sum} (gray, solid), leading to the conclusion

$$w^2_{sum} = w^2_{gating} + w^2_{shot} \quad \text{with} \quad w^2_{shot} = \text{constant} \tag{7}$$

The independence of w^2_{shot} of the absolute value of k_{OC} (but not of the ratio k_{OC}/k_{CO}) seems to be a contradiction to Figs. 1a and 2b. In Fig. 2b, the difference between the histograms with and without shot noise decreases with decreasing k_{OC}. This apparent contradiction is resolved considering that w^2 is plotted in Fig. 2c for k_{OC} being higher than the filter frequency of 50 kHz. The independence arises from the mathematics of the Poisson distribution (Eq. 1 with $F = 1$): Assume that the filter averages over M data points with nonzero current and that there are m sections (open events) with M/m data points. The

variance of the noise is $\sigma^2(M/m) = mF/M$ per section (Eq. 1). Averaging by the filter over those m sections results in $\sigma^2(M) = (mF/M)/m = F/M$ (Eq. 1). Thus, the shot noise is determined only by the number of current-carrying data points in the integration interval of the filter and not by the absolute values of the rate constants of gating (which determine m).

Consequently, the value of filtered shot noise is gating-independent (if the ratio k_{CO}/k_{OC} is kept constant) as it also holds for the baseline noise. Instead of modeling the transported charge per individual open event as done in the simulation routine described above (Fig. 1a), the amplitude histogram with shot noise could also have been calculated by convolution. This (in contrast to baseline noise) has to be done only for the apparent open peak of the histogram. However, convolution is also very time-consuming; thus, it was found to be simpler to use the simulation program as described above. Nevertheless, Fig. 2c shows that the simulation program has worked properly.

The gating independence of the shot noise signal at the output of the low-pass filter provides the following explanation of the results in Fig. 2a, b. In Fig. 2b, the difference of the histograms with and without shot noise becomes smaller with decreasing rate constants. This corresponds to the fact that the width w is the root of the squares in Eq. 7; thus, w becomes insensitive to the constant w^2_{shot} with increasing w^2_{gating}. In Fig. 2a, the nominal current i_0 decreases with the inverse of the rate constants T in order to fulfill Eq. 2 for constant $n = 10$. Consequently, w_{shot} is no longer constant and leads to higher shot noise with decreasing rate constants (Eq. 1).

For the experimenter considering whether shot noise has to be accounted for in the gating analysis, the situation in Fig. 2b is relevant: An apparent single-channel current I_{app} is measured. The missing component in Fig. 2 is the baseline noise. Including the baseline noise, time series of sufficient length (up to 10^8 sampling intervals of 5 μs) were generated from the two-state Markov model of Eq. 5 with and without shot noise. Simulations included average currents i_0 of 4.8, 16 and 48 pA and noise (σ_B) of 1, 0.3 or 0.1 pA. This provides a survey of likely and desirable experimental conditions. k_{CO} again was $5 \cdot k_{OC}$, resulting in an apparent single-channel current $I_{app} = 5/6 \cdot i_0$ for high gating frequencies. The selected values of k_{OC} ranged between 1 ms^{-1} and 30 μs^{-1}.

From the simulated time series, amplitude histograms like those in Fig. 2a,b were generated. Four of them are displayed in Fig. 3. The solid lines give the amplitude histograms with shot noise; the dashed lines give those without shot noise. It is obvious that the amplitude histograms with shot noise are slightly broader than those without. The two histograms in the middle, "4 μs^{-1} without shot noise" and "10 μs^{-1} with shot noise,"

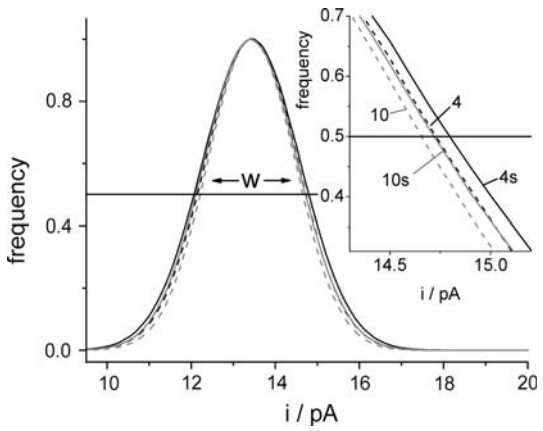

Fig. 3 Amplitude histograms simulated for two different values of k_{OC} with and without shot noise for $i_0 = 16$ pA and $\sigma_B = 1$ pA. Filter cut-off frequency was 50 kHz. *Horizontal bars* illustrate the determination of w. *Inset* gives an enlarged presentation of the differences and provides the assignment to the values of k_{OC} (4 and 10 μs^{-1}, as indicated by the numbers) and to the presence (*solid lines*, index s) and absence (*dashed lines*, without index) of shot noise

coincide. This illustrates the influence of ignoring the shot noise in the analysis: If the researcher assumes that there is no shot noise, fitting of the curve in the middle would result in $k_{OC} = 4$ μs^{-1}. If shot noise were included in the analysis, fitting would deliver the value of 10 μs^{-1}. Furthermore, Fig. 3 demonstrates the requirement of excellent baseline recordings because an error in the determination of the baseline noise would override the small differences between the histograms at very high gating frequencies.

In order to show the results of many simulations in a more compact way, the amplitude histograms are presented by the values of w in Fig. 4. w is the FWHM determined along the horizontal line in Fig. 3.

First, the simulations without shot noise (open symbols in Fig. 4, dashed curve) yield a good illustration of a previous investigation showing what gating frequencies can be revealed by analysis of beta distributions in the absence of shot noise (Schroeder and Hansen 2006). As long as the width w decreases with the rate constant given at the abscissa, this rate constant (and the related k_{CO}) can be revealed from a fit of the amplitude histogram (Schroeder and Hansen 2006). The decay of the width of the amplitude histograms is limited by the noise of the recording apparatus (horizontal lines), demonstrating that the signal-to-noise ratio is the crucial determinant of temporal resolution. The more steeply the curve decays, the better is the accuracy of the determination of the rate constants. The curves illustrate the intriguing feature that under good conditions (Fig. 4b) rate constants of up to 10 μs^{-1} can be determined in signals filtered by a 50-kHz four-pole Bessel filter. If fantastic amplifiers were available with noise of 0.1 pA, then rate constants of 100 μs^{-1} could be reached at

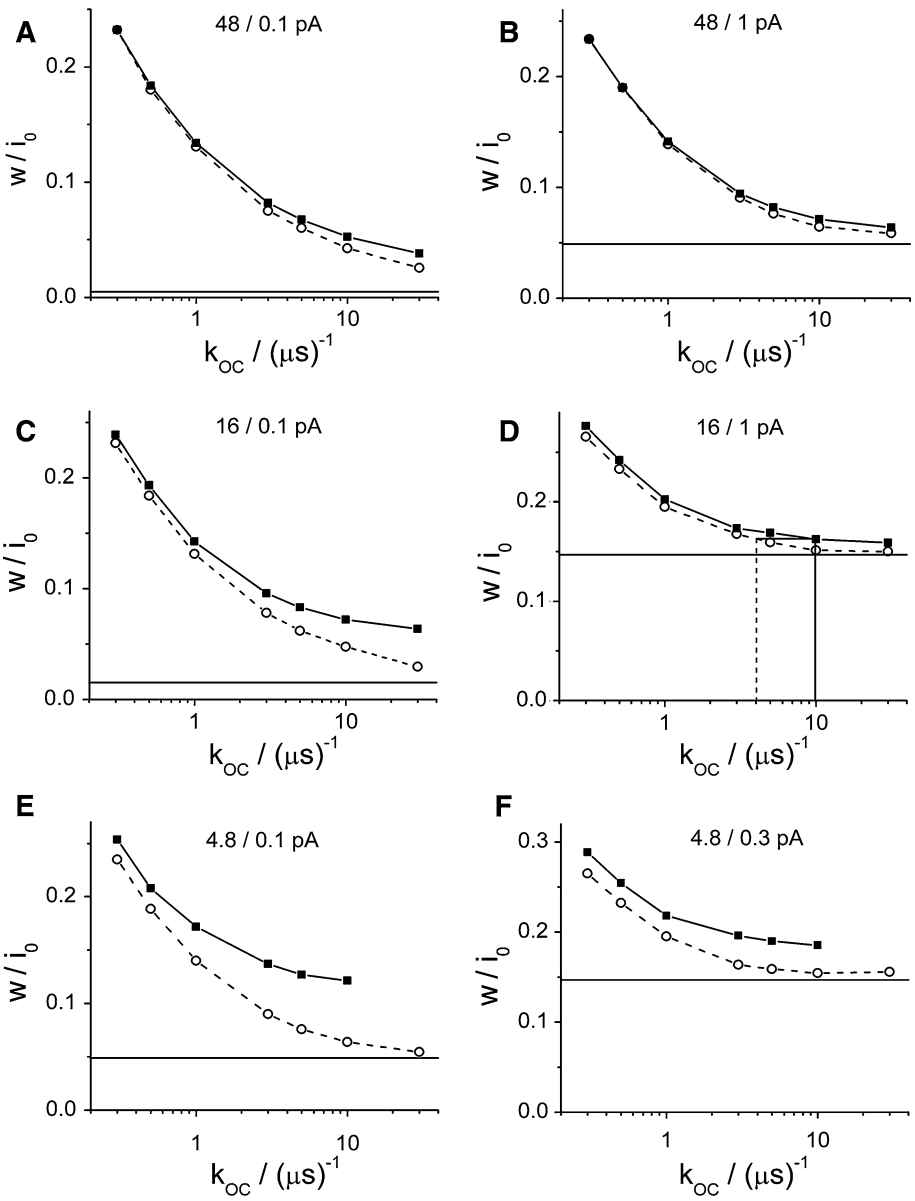

Fig. 4 Width of the amplitude histograms like those in Figs. 2 and 3 at half-maximum frequency (FWHM = w) obtained from time series simulated from a C-O model with fast gating ($k_{OC} = 1/\tau_O$ is given at the abscissa, $k_{CO} = 5 \cdot k_{OC}$). The widths are normalized to the nominal current i_0. Numbers above the curves give i_0/σ_B. *Solid horizontal lines* in each graph represent the baseline noise ($w_{Gauss} = 2.35\sigma$). *Closed symbols* connected by solid lines were generated with shot noise; *open symbols* connected by dashed lines were generated without shot noise. "Experimental" conditions as in Figs. 2 and 3. The influence of shot noise on the estimation of the rate constants is demonstrated in **d** by drawing *horizontal lines*. **d** *Vertical solid line* at $k_{OC} = 10\ \mu s^{-1}$ marks the rate constant which is obtained if shot noise is accounted for in the analysis. $k_{OC} = 4\ \mu s^{-1}$ is obtained if shot noise is ignored (*dashed vertical line*)

high single-channel currents (Fig. 4a, the curve is still decaying at 30 μs^{-1}). In MaxiK, currents of 160 pA were found at 250 mV in 3.4 M K^+ (Brelidze et al. 2003).

Second, the simulations with shot noise (closed squares, solid black curve) show that the decay of w with k_{OC} is less steep than that without shot noise. The difference between the curves with and without shot noise increases with k_{CO}. This becomes obvious from an inspection of the derivation of Eq. 7 (expanded by the inclusion of $w^2_{baseline}$):

$$\frac{\partial w_{sum}}{\partial w_{shot}} = -\frac{w_{shot}}{\sqrt{w^2_{gating} + w^2_{baseline} + w^2_{shot}}} \qquad (8)$$

With w^2_{gating} becoming smaller at increasing k_{OC}, the absolute value of $\partial w_{sum}/\partial w_{shot}$ increases. Of course, $\partial w_{sum}/\partial w_{shot}$ applies only for incrementally small differences; however, it indicates the tendency, and the correct values are obtained by simulation.

In Fig. 4d, the increase of the difference between the dashed and the solid lines is not observed. If $w_{baseline}$ becomes greater than w_{gating}, then the denominator of Eq. 8 (and thus $\partial w_{sum}/\partial w_{shot}$) becomes more and more independent of w_{gating}. A similar effect is also found when Fig. 4e is compared with 4f.

For the simulations with 4.8 pA (Fig. 4e, f), the point at 30 μs^{-1} with shot noise has been omitted because the average number of ions passing per mean open event is 1 (Eq. 2 for $T = 1/k_{OC}$). Replacing Eq. 3 by an algorithm that can handle expected ion numbers below 1 is useless at the present time as it is not known how the channel dynamics handle noninteger numbers of ions, i.e., whether

and how the interplay between protein dynamics and ion movement is synchronized to achieve transport of an integer number of ions.

Discussion

There are two important messages in the graphs of Fig. 4. First, they contain the convincing message that the analysis of amplitude histograms, indeed, can reveal rate constants which are by a factor of 200 above the corner frequency of the filter. After gating has become so fast that the closed and open levels are merged into one apparent open level (I_{app}) (Schroeder and Hansen 2006), the histograms become narrower with increasing rate constants (Fig. 2a, b). Rate constants can be determined from the histograms until the curves in Fig. 4 merge with baseline noise at k_{OC} above 10 μs^{-1}, depending on the signal-to-noise ratio. Second, shot noise does not have a severe influence on the evaluation.

Among the examples displayed above, only those with noise of 1 pA come close to what can be found in real experiments. Also, this value can be reached only under optimal conditions like minimizing pipette capacitance by internal coating of the pipettes with sigmacote and drawing it close to the surface of the bathing medium (Farokhi et al. 2000), heating the coated pipettes overnight at 55°C (Huth et al. 2008), covering the water surface with oil (Levis and Rae 1992) or using quartz pipettes (Parzefall et al. 1998) and employing the integrating mode of the amplifier. Even under those optimal conditions, the influence of the shot noise is very small.

The short horizontal line in Fig. 4d illustrates the error in the determination of the rate constants that can result from ignoring the shot noise. This horizontal line is an alternative presentation of the situation shown in Fig. 3: The evaluation of a measured amplitude histogram leads to $w = 0.1625$ (normalized to i_0). This value of w is marked by the horizontal line in Fig. 4d. It meets the curves with and without shot noise at different values of k_{OC}. The related vertical lines show the rate constant that would be evaluated by a fitting routine. If the fitting routine accounts for shot noise, then it delivers a rate constant $k_{OC} = 10\ \mu s^{-1}$. If the shot noise were ignored in the analysis, a value of 4 μs^{-1} would be obtained.

Whether or not the rate constant $k_{CO} = 5\ k_{OC}$ can be obtained from the analysis depends on the skewness of the amplitude histograms, which may be weak because in the range above 1 μs^{-1} the shape becomes quite gaussian. In order to answer this question, the fits have to be repeated with different values of i_0 (determining k_{CO} via Eq. 6) and it has to be investigated whether the error sum plotted versus i_0 exhibits a minimum (Schroeder and Hansen 2006).

The different values of k_{OC} obtained with and without shot noise may be regarded as a severe error. However, under realistic experimental conditions, this effect may not be the major problem of the exact evaluation of rate constants. The scatter of the determination of the rate constants in this range was found to be a factor of 1.5–3.5 (in extreme cases, up to 6) (Schroeder and Hansen 2007), and this random error may override the systematic error of neglecting shot noise. Eliminating the random error by a very high number of experiments may become extremely time-consuming since only a minor part of the time series provides the required stability of the seal (as indicated by artifact-free baselines) and because the fit of a single histogram may take several hours. This random error does not come as a surprise considering how flat the curves in Fig. 4 are in the range around 10 μs^{-1}. The accuracy necessary to realize an influence of the shot noise on the determination of rate constants would require much higher experimental efforts, which probably cannot be met. For instance, lowering the scatter of the determination of rate constants from amplitude histograms would require very smooth histograms, which have to be taken from records of the time series much longer than the 10 s used by Schroeder and Hansen (2007, 2008). This extension of the recording time is limited by the requirement of stationary patches of extreme lifetimes.

The incorporation of shot noise in the analysis will become important if the quality of the patch-clamp amplifiers improves. Then, not only the range of analyzable rate constants will increase but also the effects of shot noise observed at 0.3 or 0.1 pA (at 50 kHz bandwidth) may become important. However, even amplifiers with a cooled headstage like the Axopatch 200B can suppress noise only to a σ_B of 145 fA at 10 kHz bandwidth (according to http://www.moleculardevices.com). At a bandwidth of 50 kHz this may lead to σ_B of slightly below 1 pA, as used in the simulations above. Thus, there has not been any dramatic improvement during recent years. However, such an improvement is very desirable if the analysis of fast gating is to be employed for testing the predictions of MD simulations.

Future low-noise amplifiers may allow for higher corner frequencies. The simulations above were done for an anti-aliasing filter of 50 kHz. Application of these results to other corner frequencies has to be done along the following rules: Let the ratio of the filter frequencies be $c = 50$ kHz/x kHz, then the results of the 50-kHz simulations hold for the x-kHz values for the following substitutions:

$$i_x = i_{50}/c \quad k_{ij,x} = k_{ij,50}/c \quad n_x = n_{50}/c \qquad (9a, b, c)$$

Another question deals with the assumption that the Poisson distribution applies to the passages of ions during an open event leading to a Fano factor of $F = 1$ (Eq. 1). A

decrease in the Fano factor could originate from a limitation of the upper number of ions per event by the minimum transfer time of an ion. However, at moderate single-channel currents, such an effect is not expected to impose a strict upper limit, as indicated by the finding in MaxiK that single-channel current can be increased dramatically by increasing potassium concentration (Schroeder and Hansen 2007), reaching 160 pA in 3.4 M K^+ solution (Brelidze et al. 2003). More important is the decrease of the Fano factor by intermediate steps in the transport cycle (Sigworth et al. 1987) or by single-file diffusion (Piccinini et al. 2007). On the other hand, the Fano factor may be greater than 1 if the net current i_0 is composed of unidirectional currents i_+ and i_- of much higher values, each of them contributing to the Fano factor. MD simulations showed that even at +100 mV there is a strong backward flow (Piccinini et al. 2007), which is not expected from classical models (Hansen et al. 1981). This high backward flow would cause a Fano factor of up to 3 at high membrane potentials if independent movement of ions were assumed.

Employing a combination of MD simulations and Monte Carlo simulations revealed that the effect of a high backward current is overcompensated by the effect of single-file diffusion and this decreases the Fano factor to $F = 0.73$ (Piccinini et al. 2007; Brunetti et al. 2007) at high membrane potentials (where the analysis of flickering is interesting) (Schroeder and Hansen 2007, 2008). The small deviation from $F = 1$ (Eq. 1) found in the simulations of Piccinini et al. (2007) and the remaining uncertainty related to such MD simulations diminish the need to adjust the above calculations for this smaller Fano factor yet.

Furthermore, the analysis here does not make assumptions about the detailed mechanism of ion transport through the channel and its activation. In the analytical approaches (e.g., Heinemann and Sigworth 1988), a reaction kinetic model of ion transport and of inactivation similar to that of Finkelstein and Andersen (1981) was used. We feel that, in light of recent results from structural analysis (Doyle 2004), it is premature to model the journey of an ion through inner pore, cavity and selectivity filter by a hypothetical reaction kinetic scheme. Such a simple kinetic lazy-state model (Hansen et al. 1983) may not apply because in the model of Schroeder and Hansen (2007) fast gating was determined by the time integral over the occupation of a sensing site (probably site S2 in the selectivity filter), indicating a parametric and not a simple kinetic relationship between state occupation and protein deformation.

Of course, a model avoiding assumptions on the coupling of gating and transport is less closely related to the biophysics of the channel, but it would apply to a wider range of putative (presently mainly unknown) mechanisms. Thus, in the studies here, gating is presented by a Markov model and ion transition is assumed to be modulated by the Poisson distribution without explicitly quantified mutual interaction.

Acknowledgement This work was supported by the Deutsche Forschungsgemeinschaft (Ha712/14-3). We are grateful to Prof. Dr. Axel Scheidig for continuous support of our work.

References

Ashcroft FM (2006) From molecule to malady. Nature 440:440–447
Benndorf K (1995) Low noise recordings. In: Sackmann B, Neher E (eds) Single channel recordings, 2nd edn. Plenum Press, London, pp 129–145
Bernèche S, Roux B (2005) A gate in the selectivity filter of potassium channels. Structure 13:91–560
Blatt MR (2004) Membrane transport in plants. Blackwell, Oxford
Blunck R, Starace DM, Correa AM, Bezanilla F (2004) Detecting rearrangements of Shaker and NaChBac in real-time with fluorescence spectroscopy in patch-clamped mammalian cells. Biophys J 86:3966–3980
Bortkewitsch VL (1898) Poissonverteilung über Pferdetritte bei preussischen Offizieren. Monatshefte Math 9:A39–A41
Brelidze TI, Niu X, Magleby KL (2003) A ring of eight conserved negatively charged amino acids doubles the conductance of BK channels and prevents inward rectification. Proc Natl Acad Sci USA 100:9017–9022
Brunetti R, Affinito F, Jacoboni C, Piccinini E, Rudan M (2007) Shot noise in single open ion channels: a computational analysis approach based on atomistic simulations. J Comput Electron 6:391–394
Compoint M, Carloni P, Ramseyer C, Girardet C (2004) Molecular dynamics study of the KcsA channel at 2.0-Å resolution: stability and concerted motions within the pore. Biochim Biophys Acta 1661:26–39
Devroye L (1986) Non-uniform random variate generation. Springer, New York. http://cg.scs.carleton.ca/~luc/rnbookindex.html. Accessed 19 Jan 2009
Doyle DA (2004) Molecular insights into ion channel function. Mol Membr Biol 21:221–225
Fano U (1947) Ionization yield of radiation II. The fluctuations of the number of ions. Phys Rev 72:26–29
Farokhi A, Keunecke M, Hansen UP (2000) The anomalous mole fraction effect in *Chara*: gating at the edge of temporal resolution. Biophys J 79:3072–3082
Feller W (1968) An introduction to probability theory and its applications, vol 1. John Wiley & Sons, New York
Finkelstein A, Andersen OS (1981) The gramicidin A channel: a review of its permeability characteristics with special reference to the single-file aspect of transport. J Membr Biol 59:155–171
FitzHugh R (1983) Statistical properties of the asymmetric random telegraph signal with application to single-channel analysis. Math Biosci 64:75–89
Freddolino PL, Liu F, Gruebele M, Schulten K (2008) Ten-microsecond molecular dynamics simulation of a fast-folding WW domain. Biophys J 94:L75–L77
Frehland E (1978) Current noise around steady states in discrete transport systems. Biophys Chem 8:255–265
Gillespie DT (1977) Exact stochastic simulation of coupled chemical reactions. J Phys Chem 81:2340–2361
Hansen UP, Gradmann D, Sanders D, Slayman CL (1981) Interpretation of current–voltage relationships for "active" ion transport systems: I. Steady-state reaction-kinetic analysis of class-I mechanisms. J Membr Biol 63:165–190

Hansen UP, Tittor J, Gradmann D (1983) Interpretation of current–voltage relationships for "active" ion transport systems: II. Nonsteady-state reaction kinetic analysis of class I mechanisms with one slow time-constant. J Membr Biol 75:141–169

Hansen UP, Cakan O, Abshagen M, Farokhi A (2003) Gating models of the anomalous mole fraction effect of single-channel current in *Chara*. J Membr Biol 192:45–63

Hedrich R, Marten I (2006) 30-year progress of membrane transport in plants. Planta 224:725–739

Heinemann SH, Sigworth FJ (1988) Open channel noise. IV. Estimation of rapid kinetics of formamide block in gramicidin A channels. Biophys J 54:757–764

Heinemann SH, Sigworth FJ (1990) Open channel noise. V. Fluctuating barriers to ion entry in gramicidin A channels. Biophys J 57:499–514

Heinemann SH, Sigworth FJ (1991) Open channel noise. VI. Analysis of amplitude histograms to determine rapid kinetic parameters. Biophys J 60:577–587

Huth T, Schmidtmayer J, Alzheimer C, Hansen UP (2008) 4-mode gating model of the inactivation of sodium channel Nav1.2a. Pfluegers Arch 457:103–119

Jeon J, Voth GA (2008) Gating of the mechanosensitive channel protein MscL: the interplay of membrane and protein. Biophys J 94:3497–3511

Katz B, Miledi R (1970) Membrane noise produced by acetylcholine. Nature 226:962–963

Kolb HA, Läuger P, Bamberg E (1975) Correlation analysis of electrical noise in lipid bilayer membranes: kinetics of gramicidin A channels. J Membr Biol 20:133–154

Lehmann-Horn F, Jurkat-Rott K (1999) Voltage-gated ion channels and hereditary disease. Physiol Rev 79:1317–1372

Levis RA, Rae JL (1992) Constructing a patch clamp set up. Methods Enzymol 207:18–66

Marsaglia G (2003) Random number generators. J Mod Appl Stat Methods 2:2–13

Miloshevsky GV, Jordan PC (2008) Conformational changes in the selectivity filter of the open-state KcsA channel: an energy minimization study. Biophys J 95:3239–3251

Neher E, Sakmann B (1976) Single-channel currents recorded from membrane of denervated frog muscle fibres. Nature 260:799–802

Neher E, Stevens CF (1977) Conductance fluctuations and ionic pores in membranes. Annu Rev Biophys Bioeng 6:345–381

Parzefall F, Wilhelm R, Heckmann M, Dudel J (1998) Single channel currents at six microsecond resolution elicited by acetylcholine in mouse myoballs. J Physiol 512:181–188

Piccinini E, Affinito F, Brunetti R, Jacoboni C, Rudan M (2007) Computational analysis of current and noise properties of a single open ion channel. J Chem Theory Comput 3:248–255

Riessner T (1998) Level detection and extended beta distributions for the analysis of fast rate constants of Markov processes in sampled data. Shaker-Verlag, Aachen

Schroeder I, Hansen UP (2006) Strengths and limits of beta distributions as a means of reconstructing the true single-channel current in patch clamp time series with fast gating. J Membr Biol 210:199–212

Schroeder I, Hansen UP (2007) Saturation and μs-gating of current indicate depletion-induced instability of the MaxiK selectivity filter. J Gen Physiol 130:83–97

Schroeder I, Hansen UP (2008) Tl^+-induced μs-gating of current indicate instability of the MaxiK selectivity filter as caused by ion/protein interaction. J Gen Physiol 131:365–378

Schroeder I, Huth T, Suitchmezian V, Jarosik J, Schnell S, Hansen UP (2004) Distributions-per-level: a means of testing level detectors and models of patch clamp data. J Membr Biol 197: 49–58

Schottky W (1918) Über spontane Stromschwankungen in verschiedenen Elektrizitätsleitern. Annu Phys (Leipzig) 57:541–567

Sigworth F (1985) Open channel noise. I. Noise in acetylcholine receptor currents suggests conformational fluctuations. Biophys J 47:709–720

Sigworth F, Urry DW, Prasad KU (1987) Open channel noise. III. High-resolution recordings show rapid current fluctuations in gramicidin A and four chemical analogues. Biophys J 52:1055–1064

Tayefeh S, Kloss T, Thiel G, Hertel B, Moroni A, Kast SM (2007) Molecular dynamics simulation of the cytosolic mouth in Kcv-type potassium channels. Biochemistry 46:4826–4839

Walden M, Accardi A, Wu F, Xu C, Williams C, Miller C (2007) Uncoupling and turnover in a Cl^-/H^+ exchange transporter. J Gen Physiol 129:317–329

Weise R, Gradmann D (2000) Effects of Na^+ on the predominant K^+ channel in the tonoplast of *Chara*: decrease of conductance by blocks in 100 ns range and induction of oligo- or poly-subconductance gating modes. J Membr Biol 175:87–93

White PJ, Ridout MS (1998) The estimation of rapid rate constants from current–amplitude frequency distributions of single-channel recordings. J Membr Biol 161:115–129

Yellen G (1984) Ionic permeation and blockade in Ca^{2+}-activated K^+ channels of bovine chromaffin cells. J Gen Physiol 84: 157–186